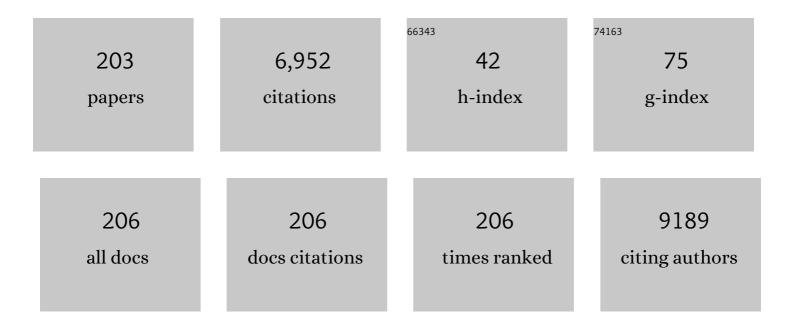
List of Publications by Year in descending order

Source: https://exaly.com/author-pdf/2153251/publications.pdf Version: 2024-02-01



#	Article	IF	CITATIONS
1	Insights into Improving Photoelectrochemical Waterâ€6plitting Performance Using Hematite Anode. Energy Technology, 2022, 10, 2100457.	3.8	10
2	Nicotiana genus: a green and sustainable source for designing of nitrogen-rich efficient carbon nanocomposites for the hydrogenation of nitrophenol and non-enzymatic glucose sensing. Materials Today Sustainability, 2022, 17, 100085.	4.1	4
3	Spatially dispersed one-dimensional carbon architecture on oxide framework for oxygen electrochemistry. Chemical Engineering Journal, 2022, 433, 133649.	12.7	10
4	Self-Assembled TMD Nanoparticles on N-Doped Carbon Nanostructures for Oxygen Reduction Reaction and Electrochemical Oxygen Sensing Thereof. ACS Applied Materials & Interfaces, 2022, 14, 5134-5148.	8.0	12
5	Interfacial Electron Transfer Strategy to Improve the Hydrogen Evolution Catalysis of CrP Heterostructure. Small, 2022, 18, e2106139.	10.0	9
6	Trimetallic oxide-hydroxide porous nanosheets for efficient water oxidation. Chemical Engineering Journal, 2022, 435, 135019.	12.7	13
7	Designed synthesis of a hierarchical MoSe ₂ @WSe ₂ hybrid nanostructure as a bifunctional electrocatalyst for total water-splitting. Sustainable Energy and Fuels, 2022, 6, 1708-1718.	4.9	7
8	Design of Hierarchical Oxide arbon Nanostructures for Trifunctional Electrocatalytic Applications. Advanced Materials Interfaces, 2022, 9, .	3.7	8
9	Modulating the Midgap States of 3D–2D Hybrid ZnO by Codoping and Its Effect on Visible Photocatalysis. Industrial & Engineering Chemistry Research, 2022, 61, 4244-4254.	3.7	2
10	FeCoNiMnCr High-Entropy Alloy Nanoparticle-Grafted NCNTs with Promising Performance in the Ohmic Polarization Region of Fuel Cells. ACS Applied Materials & Interfaces, 2022, 14, 16108-16116.	8.0	23
11	MoS2/SnO2 heterojunction-based self-powered photodetector. Applied Physics Letters, 2022, 120, .	3.3	9
12	Enhancement of Photoresponsivity of β-In ₂ S ₃ /Si Broadband Photodetector by Decorating With Reduced-Graphene Oxide. IEEE Transactions on Electron Devices, 2022, 69, 4355-4361.	3.0	2
13	Current Insight into 3D Printing in Solidâ€State Lithiumâ€Ion Batteries: A Perspective. Batteries and Supercaps, 2022, 5, . Electrically Modulated Wavelength-Selective Photodetection Enabled by <mml:math< td=""><td>4.7</td><td>19</td></mml:math<>	4.7	19
14	xmlns:mml="http://www.w3.org/1998/Math/MathML" display="inline" overflow="scroll"> <mml:msub><mml:mrow><mml:mi>Mo</mml:mi><mml:mi mathvariant="normal">S</mml:mi </mml:mrow><mml:mn>2</mml:mn></mml:msub> <mml:mo>/</mml:mo> <r mathvariant="normal">OHeterostructure. Physical Review</r 	nmi:mrow	v><11 mml:mi>Z
15	Applied, 2022, 17, . Electronic structure modulation of molybdenum-iron double-atom catalyst for bifunctional oxygen electrochemistry. Chemical Engineering Journal, 2022, 449, 137705.	12.7	14
16	Universal avenue to metal-transition metal carbide grafted N-doped carbon framework as efficient dual Mott-Schottky electrocatalysts for water splitting. Sustainable Materials and Technologies, 2022, 33, e00451.	3.3	10
17	High-entropy alloys for water oxidation: a new class of electrocatalysts to look out for. Chemical Communications, 2021, 57, 611-614.	4.1	33
18	Ruthenium nanodendrites on reduced graphene oxide: an efficient water and 4-nitrophenol reduction catalyst. New Journal of Chemistry, 2021, 45, 1556-1564.	2.8	13

#	Article	IF	CITATIONS
19	Atomic Arrangement Modulation in CoFe Nanoparticles Encapsulated in N-Doped Carbon Nanostructures for Efficient Oxygen Reduction Reaction. ACS Applied Materials & Interfaces, 2021, 13, 3771-3781.	8.0	28
20	Review on recent progress in metal–organic framework-based materials for fabricating electrochemical glucose sensors. Journal of Materials Chemistry B, 2021, 9, 7927-7954.	5.8	55
21	<i>In situ</i> self-organization of uniformly dispersed Co–N–C centers at moderate temperature without a sacrificial subsidiary metal. Green Chemistry, 2021, 23, 3115-3126.	9.0	24
22	Mechanistic study on nitrogen-doped graphitic carbon-reinforced chromium nitride as a durable electrocatalyst for oxygen reduction. Journal of Materials Chemistry A, 2021, 9, 16575-16584.	10.3	14
23	The Untold Tale of the ORR Polarization Curve. Journal of Physical Chemistry C, 2021, 125, 10378-10385.	3.1	15
24	Identifying the Accuracy of Various Approaches for Determining the Fraction of Surface Atoms in a Nanoparticle to Deepen Students' Understanding of Size-Dependent Properties. Journal of Chemical Education, 2021, 98, 1982-1987.	2.3	3
25	Solution-Processed SnSe ₂ –RGO-Based Bulk Heterojunction for Self-Powered and Broadband Photodetection. ACS Applied Electronic Materials, 2021, 3, 3131-3138.	4.3	12
26	Electrical transport modulation of VO2/Si(111) heterojunction by engineering interfacial barrier height. Journal of Applied Physics, 2021, 129, .	2.5	7
27	Asymmetric Supercapacitors with Nanostructured RuS ₂ . Energy & Fuels, 2021, 35, 12671-12679.	5.1	8
28	Overcoming the Challenges Associated with the InN/InGaN Heterostructure via a Nanostructuring Approach for Broad Band Photodetection. ACS Applied Electronic Materials, 2021, 3, 4243-4253.	4.3	4
29	Differentiation of ultraviolet/visible photons from near infrared photons by MoS2/GaN/Si-based photodetector. Applied Physics Letters, 2021, 119, .	3.3	19
30	pH-dependent hydrogen evolution using spatially confined ruthenium on hollow N-doped carbon nanocages as a Mott–Schottky catalyst. Journal of Materials Chemistry A, 2021, 9, 13958-13966.	10.3	40
31	Robust Visible-Blind Wearable Infrared Sensor Based on IrP2 Nanoparticle-Embedded Few-Layer Graphene and the Effect of Photogating. ACS Applied Materials & Interfaces, 2021, 13, 54258-54265.	8.0	0
32	Inhomogeneity-mediated systematic reduction of the Schottky barrier in a Au/GaN nanorod film interface. Semiconductor Science and Technology, 2021, 36, 015017.	2.0	3
33	Uniform Distribution of Ruthenium Nanoparticles on Nitrogen-Doped Carbon Nanostructure for Oxygen Reduction Reaction. ACS Applied Energy Materials, 2021, 4, 12191-12200.	5.1	5
34	Defect and strain modulated highly efficient ZnO UV detector: Temperature and low-pressure dependent studies. Applied Surface Science, 2020, 505, 144365.	6.1	46
35	On the origin of metallicity and stability of the metastable phase in chemically exfoliated MoS2. Applied Materials Today, 2020, 19, 100544.	4.3	8
36	Harvesting energy via stimuliâ€free water/moisture dissociation by mesoporous SnO ₂ –based hydroelectric cell and CuO as a pump for atmospheric moisture. International Journal of Energy Research, 2020, 44, 1276-1283.	4.5	11

#	Article	IF	CITATIONS
37	Alkaline earth metal based single atom catalyst for the highly durable oxygen reduction reaction. Applied Materials Today, 2020, 21, 100846.	4.3	16
38	Construction of noble-metal alloys of cobalt confined N-doped carbon polyhedra toward efficient water splitting. Green Chemistry, 2020, 22, 7884-7895.	9.0	56
39	Temperature-Dependent Electrical Transport and Optoelectronic Properties of SnS ₂ /p-Si Heterojunction. ACS Applied Electronic Materials, 2020, 2, 2155-2163.	4.3	23
40	Inner Sphere Electron Transfer Promotion on Homogeneously Dispersed Fe-N <i>_x</i> Centers for Energy-Efficient Oxygen Reduction Reaction. ACS Applied Materials & Interfaces, 2020, 12, 36026-36039.	8.0	39
41	Energy-Efficient Rational Designing of Multifunctional Nanocomposites by Preferential Anchoring of Metal Ions via Fermi Level Positioning of Carbon Nanostructures. ACS Applied Materials & Interfaces, 2020, 12, 53749-53759.	8.0	8
42	Temperature Dependent "S-Shaped―Photoluminescence Behavior of InGaN Nanolayers: Optoelectronic Implications in Harsh Environment. ACS Applied Nano Materials, 2020, 3, 8453-8460.	5.0	9
43	Device Architecture for Visible and Near-Infrared Photodetectors Based on Two-Dimensional SnSe2 and MoS2: A Review. Micromachines, 2020, 11, 750.	2.9	19
44	Self-Organized Single-Atom Tungsten Supported on the N-Doped Carbon Matrix for Durable Oxygen Reduction. ACS Applied Materials & Interfaces, 2020, 12, 43586-43595.	8.0	29
45	Self-powered, ultrasensitive, room temperature humidity sensors using SnS2 nanofilms. Scientific Reports, 2020, 10, 14611.	3.3	20
46	Unique One-Step Strategy for Nonmetallic and Metallic Heteroatom Doped Carbonaceous Materials. ACS Omega, 2020, 5, 32852-32860.	3.5	16
47	Defect-Mediated Transport in Self-Powered, Broadband, and Ultrafast Photoresponse of a MoS ₂ /AlN/Si-Based Photodetector. ACS Applied Electronic Materials, 2020, 2, 944-953.	4.3	40
48	Different types of band alignment at MoS2/(Al, Ga, In)N heterointerfaces. Applied Physics Letters, 2020, 116, .	3.3	16
49	Highly Responsive, Self-Powered <i>a</i> -GaN Based UV-A Photodetectors Driven by Unintentional Asymmetrical Electrodes. ACS Applied Electronic Materials, 2020, 2, 769-779.	4.3	31
50	Next-generation self-powered and ultrafast photodetectors based on III-nitride hybrid structures. APL Materials, 2020, 8, .	5.1	30
51	Giant enhancement in photoresponse via engineering of photo-induced charge (electron and hole) transfer in linear and non-linear devices. Sensors and Actuators A: Physical, 2020, 304, 111842.	4.1	6
52	Mechanistic Investigation into Efficient Water Oxidation by Co–Ni-Based Hybrid Oxide–Hydroxide Flowers. ACS Applied Materials & Interfaces, 2020, 12, 13888-13895.	8.0	31
53	Dual roles of a transparent polymer film containing dispersed N-doped carbon dots: A high-efficiency blue light converter and UV screen. Applied Surface Science, 2020, 510, 145405.	6.1	36
54	Nickel in nitrogen-doped graphene nanotube as efficient electrocatalyst for water splitting. AIP Conference Proceedings, 2020, , .	0.4	0

#	Article	IF	CITATIONS
55	ZnO hybrid microstructures as dark catalyst. AIP Conference Proceedings, 2019, , .	0.4	1
56	Unconventional energy transfer from narrow to broad luminescent wide band gap materials. Europhysics Letters, 2019, 127, 17003.	2.0	1
57	"Rinse, Repeatâ€: An Efficient and Reusable SERS and Catalytic Platform Fabricated by Controlled Deposition of Silver Nanoparticles on Cellulose Paper. ACS Sustainable Chemistry and Engineering, 2019, 7, 14089-14101.	6.7	54
58	Double Gaussian distribution of barrier heights and self-powered infrared photoresponse of InN/AIN/Si (111) heterostructure. Journal of Applied Physics, 2019, 126, .	2.5	19
59	In Situ Decoration of Ultrafine Ru Nanocrystals on N-Doped Graphene Tube and Their Applications as Oxygen Reduction and Hydrogen Evolution Catalyst. ACS Applied Energy Materials, 2019, 2, 7330-7339.	5.1	32
60	Highly Responsive ZnO/AlN/Si Heterostructure-Based Infrared- and Visible-Blind Ultraviolet Photodetectors With High Rejection Ratio. IEEE Transactions on Electron Devices, 2019, 66, 1345-1352.	3.0	17
61	Photodetection Properties of Nonpolar aâ€Plane GaN Grown by Three Approaches Using Plasmaâ€Assisted Molecular Beam Epitaxy. Physica Status Solidi (A) Applications and Materials Science, 2019, 216, 1900171.	1.8	17
62	Expanding Interlayer Spacing in MoS ₂ for Realizing an Advanced Supercapacitor. ACS Energy Letters, 2019, 4, 1602-1609.	17.4	195
63	Investigation of electrical, mechanical, and thermal properties of functionalized multiwalled carbon nanotubesâ€reduced graphene Oxide/PMMA hybrid nanocomposites. Polymer Engineering and Science, 2019, 59, 1075-1083.	3.1	14
64	Self-Powered, Broad Band, and Ultrafast InGaN-Based Photodetector. ACS Applied Materials & Interfaces, 2019, 11, 10418-10425.	8.0	61
65	Photon-Free Degradation of Dyes by Ge/GeO ₂ Porous Microstructures. ACS Sustainable Chemistry and Engineering, 2019, 7, 6611-6618.	6.7	14
66	Pd-coated Ru nanocrystals supported on N-doped graphene as HER and ORR electrocatalysts. Chemical Communications, 2019, 55, 13928-13931.	4.1	51
67	Toward a Fast and Highly Responsive SnSe ₂ -Based Photodiode by Exploiting the Mobility of the Counter Semiconductor. ACS Applied Materials & amp; Interfaces, 2019, 11, 6184-6194.	8.0	39
68	Effective Surface Area Tuning of Noble Metal-Free CuBO ₂ /rGO Nanohybrid for Efficient Hydrogen Production with "On–Off―Switching. ACS Applied Energy Materials, 2019, 2, 260-268.	5.1	18
69	Non-Precious Bimetallic CoCr Nanostructures Entrapped in Bamboo-Like Nitrogen-Doped Graphene Tube As a Robust Bifunctional Electrocatalyst for Total Water Splitting. ACS Applied Energy Materials, 2018, 1, 1116-1126.	5.1	41
70	A comprehensive analysis and rational designing of efficient Fe-based oxygen electrocatalysts for metal–air batteries. Journal of Materials Chemistry A, 2018, 6, 8537-8548.	10.3	39
71	Enhanced Solar Light Absorption and Photoelectrochemical Conversion Using TiN Nanoparticle-Incorporated C ₃ N ₄ –C Dot Sheets. ACS Applied Materials & Interfaces, 2018, 10, 2460-2468.	8.0	64
72	Ultrafast-Versatile-Domestic-Microwave-Oven Based Graphene Oxide Reactor for the Synthesis of Highly Efficient Graphene Based Hybrid Electrocatalysts. ACS Sustainable Chemistry and Engineering, 2018, 6, 4037-4045.	6.7	11

#	Article	IF	CITATIONS
73	In-Plane Anisotropic Photoconduction in Nonpolar Epitaxial <i>a</i> -Plane GaN. ACS Applied Materials & Interfaces, 2018, 10, 16918-16923.	8.0	33
74	Temperature sensing using sulfur-doped carbon nanoparticles. Carbon, 2018, 133, 200-208.	10.3	27
75	Large scale synthesis of reduced graphene oxide using ferrocene and HNO3. Materials Letters, 2018, 211, 335-338.	2.6	10
76	MgO Nanocubes as Self-Calibrating Optical Probes for Efficient Ratiometric Detection of Picric Acid in the Solid State. ACS Sustainable Chemistry and Engineering, 2018, 6, 13719-13729.	6.7	17
77	In Situ Fabrication of a Nickel/Molybdenum Carbide-Anchored N-Doped Graphene/CNT Hybrid: An Efficient (Pre)catalyst for OER and HER. ACS Applied Materials & Interfaces, 2018, 10, 35025-35038.	8.0	185
78	Reduced graphene oxide-based broad band photodetector and temperature sensor: effect of gas adsorption on optoelectrical properties. Journal of Nanoparticle Research, 2018, 20, 1.	1.9	14
79	<i>Anthocephalus cadamba</i> shaped FeNi encapsulated carbon nanostructures for metal–air batteries as a resilient bifunctional oxygen electrocatalyst. Journal of Materials Chemistry A, 2018, 6, 20411-20420.	10.3	67
80	Effect of inhomogeneous mesoporosity and defects on the luminescent properties of slanted silicon nanowires prepared by facile metal-assisted chemical etching. Journal of Applied Physics, 2018, 124, 104303.	2.5	9
81	Note: Simultaneous water quality monitoring and degradation of hazardous organic pollutants. Review of Scientific Instruments, 2018, 89, 096102.	1.3	5
82	Green synthesis of MoS ₂ nanoflowers for efficient degradation of methylene blue and crystal violet dyes under natural sun light conditions. New Journal of Chemistry, 2018, 42, 14318-14324.	2.8	65
83	CoFe Nanoalloys Encapsulated in N-Doped Graphene Layers as a Pt-Free Multifunctional Robust Catalyst: Elucidating the Role of Co-Alloying and N-Doping. ACS Sustainable Chemistry and Engineering, 2018, 6, 12736-12745.	6.7	50
84	An Extrinsic Approach Toward Achieving Fast Response and Selfâ€Powered Photodetector. Physica Status Solidi (A) Applications and Materials Science, 2018, 215, 1800470.	1.8	20
85	An efficient on-board metal-free nanocatalyst for controlled room temperature hydrogen production. Chemical Science, 2017, 8, 2994-3001.	7.4	36
86	Phosphine-free avenue to Co ₂ P nanoparticle encapsulated N,P co-doped CNTs: a novel non-enzymatic glucose sensor and an efficient electrocatalyst for oxygen evolution reaction. Green Chemistry, 2017, 19, 1327-1335.	9.0	141
87	A unique approach to designing resilient bi-functional nano-electrocatalysts based on ultrafine bimetallic nanoparticles dispersed in carbon nanospheres. Journal of Materials Chemistry A, 2017, 5, 10544-10553.	10.3	33
88	Facile synthesis of ultrafine Ru nanocrystal supported N-doped graphene as an exceptional hydrogen evolution electrocatalyst in both alkaline and acidic media. Sustainable Energy and Fuels, 2017, 1, 1028-1033.	4.9	46
89	Designing Dual Emissions via Co-doping or Physical Mixing of Individually Doped ZnO and Their Implications in Optical Thermometry. ACS Applied Materials & Interfaces, 2017, 9, 16305-16312.	8.0	46
90	White Light Emission from Black Germanium. ACS Photonics, 2017, 4, 1722-1729.	6.6	11

6

#	Article	IF	CITATIONS
91	Ultrahigh-sensitive optical temperature sensing based on quasi-thermalized green emissions from Er:ZnO. Physical Chemistry Chemical Physics, 2017, 19, 2346-2352.	2.8	31
92	Red emitting Eu:ZnO nanorods for highly sensitive fluorescence intensity ratio based optical thermometry. Journal of Materials Chemistry C, 2017, 5, 1074-1082.	5.5	76
93	Thioacetamide-derived nitrogen and sulfur co-doped carbon nanoparticles used for label-free detection of copper(<scp>ii</scp>) ions and bioimaging applications. New Journal of Chemistry, 2017, 41, 13742-13746.	2.8	8
94	Maximizing the utilization of Fe–N _x C/CN _x centres for an air-cathode material and practical demonstration of metal–air batteries. Journal of Materials Chemistry A, 2017, 5, 20252-20262.	10.3	46
95	Negative-charge-functionalized carbon nanodot: a low-cost smart cold emitter. Nanotechnology, 2017, 28, 395705.	2.6	1
96	Facile and one-step synthesis of a free-standing 3D MoS ₂ –rGO/Mo binder-free electrode for efficient hydrogen evolution reaction. Journal of Materials Chemistry A, 2017, 5, 18081-18087.	10.3	39
97	Reduced graphene oxide film based highly responsive infrared detector. Materials Research Express, 2017, 4, 085603.	1.6	8
98	Rational geometrical engineering of palladium sulfide multi-arm nanostructures as a superior bi-functional electrocatalyst. Nanoscale, 2017, 9, 12628-12636.	5.6	16
99	Band Gap Engineering of Hexagonal SnSe2 Nanostructured Thin Films for Infra-Red Photodetection. Scientific Reports, 2017, 7, 15215.	3.3	102
100	Sequential Elemental Dealloying Approach for the Fabrication of Porous Metal Oxides and Chemiresistive Sensors Thereof for Electronic Listening. ACS Applied Materials & Interfaces, 2017, 9, 41428-41434.	8.0	27
101	Mechanistic view on efficient photodetection by solvothermally reduced graphene oxide. Journal of Materials Science: Materials in Electronics, 2017, 28, 14818-14826.	2.2	9
102	Designing N-doped carbon nanotubes and Fe–Fe ₃ C nanostructures co-embedded in B-doped mesoporous carbon as an enduring cathode electrocatalyst for metal–air batteries. Journal of Materials Chemistry A, 2017, 5, 16843-16853.	10.3	83
103	Experimental evidence on RH-dependent crossover from an electronic to protonic conduction with an oscillatory behaviour. Applied Physics Letters, 2017, 110, .	3.3	15
104	Enhanced UV Photodetector Response of ZnO/Si With AlN Buffer Layer. IEEE Transactions on Electron Devices, 2017, 64, 4161-4166.	3.0	25
105	Direct synthesis of Pt-free catalyst on gas diffusion layer of fuel cell and usage of high boiling point fuels for efficient utilization of waste heat. Applied Energy, 2017, 205, 1050-1058.	10.1	20
106	Effects of nanoscale morphology and defects in oxide: optoelectronic functions of zinc oxide nanowires. Radiation Effects and Defects in Solids, 2016, 171, 22-33.	1.2	9
107	A noble and single source precursor for the synthesis of metal-rich sulphides embedded in an N-doped carbon framework for highly active OER electrocatalysts. Dalton Transactions, 2016, 45, 6352-6356.	3.3	33
108	Understanding the ammonia sensing behavior of filter coffee powder derived N-doped carbon nanoparticles using the Freundlich-like isotherm. Journal of Materials Chemistry A, 2016, 4, 8860-8865.	10.3	19

#	Article	IF	CITATIONS
109	One-step, integrated fabrication of Co2P nanoparticles encapsulated N, P dual-doped CNTs for highly advanced total water splitting. Nano Energy, 2016, 30, 303-311.	16.0	195
110	Strong Red Luminescent Twin ZnO Nanorods for Nano-thermometry Application. MRS Advances, 2016, 1, 869-874.	0.9	2
111	Understanding of nitrogen-doped carbon nanoparticles based solid phosphors for white light emitting diodes. RSC Advances, 2016, 6, 67751-67755.	3.6	3
112	Temperature-Dependent Photoluminescence of g-C ₃ N ₄ : Implication for Temperature Sensing. ACS Applied Materials & Interfaces, 2016, 8, 2181-2186.	8.0	140
113	Nitrogen-assisted electroless assembling of 3D nanodendrites consisting of Pd and N-doped carbon nanoparticles as bifunctional catalysts. Green Chemistry, 2016, 18, 2115-2121.	9.0	28
114	Boron-doped carbon nanoparticles: Size-independent color tunability from red to blue and bioimaging applications. Carbon, 2016, 96, 166-173.	10.3	59
115	Au Nanocomposite Based Chemiresistive Ammonia Sensor for Health Monitoring. ACS Sensors, 2016, 1, 55-62.	7.8	148
116	Prussian blue as a single precursor for synthesis of Fe/Fe ₃ C encapsulated N-doped graphitic nanostructures as bi-functional catalysts. Green Chemistry, 2016, 18, 427-432.	9.0	152
117	Enhanced photocatalytic activity of ultra-high aspect ratio ZnO nanowires due to Cu induced defects. Radiation Effects and Defects in Solids, 2015, 170, 939-944.	1.2	1
118	Hetero-atom doped carbon nanotubes for dye degradation and oxygen reduction reaction. AIP Conference Proceedings, 2015, , .	0.4	0
119	Air stable iron/iron carbide magnetic nanoparticles embedded in amorphous carbon globules. AIP Conference Proceedings, 2015, , .	0.4	0
120	Evaporation-condensation synthesis and optical property of In2O3 octahedrons. AIP Conference Proceedings, 2015, , .	0.4	0
121	Boron and Nitrogen Co-doped Carbon Nanoparticles as Photoluminescent Probes for Selective and Sensitive Detection of Picric Acid. Journal of Physical Chemistry C, 2015, 119, 13138-13143.	3.1	100
122	Luminescence from wide band gap materials and their applications. Advances in Natural Sciences: Nanoscience and Nanotechnology, 2015, 6, 015002.	1.5	10
123	Uninterrupted galvanic reaction for scalable and rapid synthesis of metallic and bimetallic sponges/dendrites as efficient catalysts for 4-nitrophenol reduction. Dalton Transactions, 2015, 44, 4215-4222.	3.3	25
124	Wide-Range Thermometry at Micro/Nano Length Scales with In ₂ O ₃ Octahedrons as Optical Probes. ACS Applied Materials & Interfaces, 2015, 7, 23481-23488.	8.0	27
125	Si-mediated fabrication of reduced graphene oxide and its hybrids for electrode materials. Green Chemistry, 2015, 17, 776-780.	9.0	4
126	Multistage effect in enhancing the field emission behaviour of ZnO branched nanostructures. Applied Physics Letters, 2014, 104, .	3.3	9

#	Article	IF	CITATIONS
127	An electrochemical method for the synthesis of few layer graphene sheets for high temperature applications. Chemical Communications, 2014, 50, 4613.	4.1	36
128	Hexamethylenetetramine mediated simultaneous nitrogen doping and reduction of graphene oxide for a metal-free SERS substrate. RSC Advances, 2014, 4, 44146-44150.	3.6	17
129	Detailed understanding of the excitation-intensity dependent photoluminescence of ZnO materials: Role of defects. Journal of Applied Physics, 2014, 115, .	2.5	20
130	Facile hydrothermal synthesis of carbon nanoparticles and possible application as white light phosphors and catalysts for the reduction of nitrophenol. RSC Advances, 2014, 4, 11481.	3.6	34
131	Nanocomposite based flexible ultrasensitive resistive gas sensor for chemical reactions studies. Scientific Reports, 2013, 3, 2082.	3.3	114
132	The dual role of Zn–acid medium for one-step rapid synthesis of M@rGO (M = Au, Pt, Pd and Ag) hybrid nanostructures at room temperature. Chemical Communications, 2013, 49, 8949.	4.1	45
133	A comparison of ZnO films deposited on indium tin oxide and soda lime glass under identical conditions. AIP Advances, 2013, 3, .	1.3	3
134	Carbon nanotube-ZnO nanowire hybrid architectures as multifunctional devices. AIP Advances, 2013, 3, 082106.	1.3	14
135	Instantaneous reduction of graphene oxide at room temperature. RSC Advances, 2013, 3, 12621.	3.6	34
136	Excellent performance of Pt-free cathode in alkaline direct methanol fuel cell at room temperature. Journal of Materials Chemistry A, 2013, 1, 3133.	10.3	35
137	Thermal oxidation strategy for the synthesis of phase-controlled GeO ₂ and photoluminescence characterization. CrystEngComm, 2013, 15, 1043-1046.	2.6	27
138	Excitation- and power-dependent photoluminescence from oxidized Ge. Materials Letters, 2013, 101, 5-8.	2.6	0
139	Mechanism for the Compressive Strain Induced Oscillations in the Conductance of Carbon Nanotubes. Physical Review Letters, 2013, 110, 095504.	7.8	7
140	Doping by diffusion of dopants from the substrate: synthesis of doped ZnO nanowires. Journal of Materials Chemistry C, 2013, 1, 1066-1069.	5.5	4
141	Various quantum mechanical concepts for confinements in semiconductor nanocrystals. Resonance, 2013, 18, 771-776.	0.3	0
142	Towards the understanding of formation of micro/nano holes of Ge/GeO2 through phase mapping. CrystEngComm, 2013, 15, 4049.	2.6	12
143	Wideâ€Range Temperature Sensing using Highly Sensitive Greenâ€Luminescent ZnO and PMMAâ€ZnO Film as a Nonâ€Contact Optical Probe. Angewandte Chemie - International Edition, 2013, 52, 11325-11328.	13.8	44
144	Ultralong ZnO nanowires: Problems and prospects. Materials Express, 2013, 3, 185-200.	0.5	2

#	Article	IF	CITATIONS
145	Uninterrupted and reusable source for the controlled growth of nanowires. Scientific Reports, 2013, 3, 1172.	3.3	11
146	Core-Shell Nanostructures: Modeling, Fabrication, Properties, and Applications. Journal of Nanomaterials, 2012, 2012, 1-2.	2.7	3
147	Electrical properties of buckled multiwalled carbon nanotube arrays in the diffusive regime. Europhysics Letters, 2012, 99, 56006.	2.0	Ο
148	Electrical breakdown of carbon nanotube devices and the predictability of breakdown position. AIP Advances, 2012, 2, .	1.3	4
149	Unusual photoresponse of indium doped ZnO/organic thin film heterojunction. Applied Physics Letters, 2012, 100, .	3.3	62
150	Electrical characteristics of multiwalled carbon nanotube arrays and influence of pressure. AIP Advances, 2012, 2, 022103.	1.3	4
151	ZnO/Poly(3,4-ethylenedioxythiophene) Poly(styrenesulfonate) Based Ultraviolet and Visible Photodetectors: Role of Defects. Materials Express, 2012, 2, 251-256.	0.5	6
152	Thermodynamic Models for the Size-dependent Melting of Nanoparticles: Different Hypotheses. Current Nanoscience, 2012, 8, 305-311.	1.2	10
153	An Efficient and Environment Friendly Universal-White-Light-Emitting ZnO Nanophosphors. Current Nanoscience, 2012, 8, 914-918.	1.2	0
154	Fabrication of Highly Dense Nanoholes by Self-Assembled Gallium Droplet on Silicon Surface. Materials Express, 2012, 2, 245-250.	0.5	3
155	Shape Transformation of ZnO Nanorods /Nanotubes at Low Temperature. Current Nanoscience, 2012, 8, 156-160.	1.2	2
156	Green synthesis of biopolymer–silver nanoparticle nanocomposite: An optical sensor for ammonia detection. International Journal of Biological Macromolecules, 2012, 51, 583-589.	7.5	295
157	Synthesis of zinc oxide porous structures by anodization with water as an electrolyte. Applied Physics A: Materials Science and Processing, 2012, 109, 151-157.	2.3	32
158	Large scale synthesis of ultralong aligned buckled multiwalled carbon nanotubes by one-step pyrolysis. CrystEngComm, 2012, 14, 7161.	2.6	1
159	Carbon nanotube mat as substrate for ZnO nanotip field emitters. RSC Advances, 2012, 2, 2713.	3.6	10
160	Recycle and reuse of substrates and the deposit materials. RSC Advances, 2012, 2, 12136.	3.6	1
161	Gas-phase synthesis of size-classified polyhedral In2O3 nanoparticles. Journal of Materials Chemistry, 2012, 22, 3133.	6.7	5
162	Tunable device properties of free-standing inorganic/organic flexible hybrid structures obtained by exfoliation. Applied Physics Letters, 2012, 100, .	3.3	14

#	Article	IF	CITATIONS
163	Size-dependent density of nanoparticles and nanostructured materials. Physics Letters, Section A: General, Atomic and Solid State Physics, 2012, 376, 3301-3302.	2.1	20
164	Anisotropic electrical transport properties of poly(methyl methacrylate) infiltrated aligned carbon nanotube mats. Applied Physics Letters, 2012, 100, .	3.3	4
165	Facile synthesis of large area porous Cu2O as super hydrophobic yellow-red phosphors. RSC Advances, 2012, 2, 3647.	3.6	42
166	Liquid-drop model for the surface energy of nanoparticles. Physics Letters, Section A: General, Atomic and Solid State Physics, 2012, 376, 1647-1649.	2.1	37
167	Evolution of crystallinity of free gold agglomerates and shape transformation. RSC Advances, 2011, 1, 568.	3.6	8
168	Near white light emission from ZnO nanostructures. Materials Research Society Symposia Proceedings, 2011, 1303, 63.	0.1	2
169	Studies towards synthesis, evolution and alignment characteristics of dense, millimeter long multiwalled carbon nanotube arrays. Beilstein Journal of Nanotechnology, 2011, 2, 293-301.	2.8	15
170	Synthesis of one-dimensional N-doped Ga2O3 nanostructures: different morphologies and different mechanisms. Bulletin of Materials Science, 2011, 34, 1331-1338.	1.7	10
171	Preparation and Optical Properties ZnO Dumb-Bell Like Microcrystals. , 2011, , .		0
172	Synthesis of Porous Cuprous Oxide (Cu[sub 2]O) on Cu Foil. , 2011, , .		1
173	On the paradoxical relation between the melting temperature and forbidden energy gap of nanoparticles. Journal of Chemical Physics, 2010, 133, 054502.	3.0	6
174	Direct White Light Nanophosphors. Key Engineering Materials, 2010, 444, 219-228.	0.4	2
175	Melting and superheating of nanowires—a nanotube approach. Nanotechnology, 2010, 21, 205701.	2.6	8
176	Size-Dependent Melting of Finite-Length Nanowires. Journal of Physical Chemistry C, 2010, 114, 14327-14331.	3.1	31
177	Excellent field emission from semialigned carbon nanofibers grown on cylindrical copper surface. Applied Physics Letters, 2009, 95, 083108.	3.3	6
178	A One‣tep Method for the Growth of Ga ₂ O ₃ â€Nanorodâ€Based Whiteâ€Lightâ€Emitting Phosphors. Advanced Materials, 2009, 21, 3581-3584.	21.0	120
179	Preparation temperature effect on the synthesis of various carbon nanostructures. Materials Science and Engineering B: Solid-State Materials for Advanced Technology, 2009, 164, 140-150.	3.5	12
180	Surface Tension and Sintering of Free Gold Nanoparticles. Journal of Physical Chemistry C, 2008, 112, 13488-13491.	3.1	52

IF # ARTICLE CITATIONS A one-step technique to prepare aligned arrays of carbon nanotubes. Nanotechnology, 2008, 19, 155602. 181 Size-Dependent Cohesive Energy and Melting Of Non-Spherical Nanoparticles., 2008, , . 182 3 Controllable resistance and temperature dependency of carbon nanotube bundles. Applied Physics 3.3 14 Letters, 2008, 93, 063105. Comment on "Size-dependent melting behavior of Zn nanowire arrays―[Appl. Phys. Lett. 88, 173114 184 3.3 14 (2006)]. Applied Physics Letters, 2007, 91, 196101. Phenomenological Predictions of Cohesive Energy and Structural Transition of Nanoparticles. Journal of Physical Chemistry B, 2006, 110, 1033-1037. 2.6 39 Bulk cohesive energy and surface tension from the size-dependent evaporation study of nanoparticles. 186 3.3 74 Applied Physics Letters, 2005, 87, 021909. Surface excitonic emission and quenching effects in ZnO nanowire/nanowall systems: Limiting effects 3.2 183 on device potential. Physical Review B, 2005, 71, . Effective mass approximation for two extreme semiconductors: Band gap of PbS and CuBr 188 2.5 76 nanoparticles. Journal of Applied Physics, 2004, 95, 5035-5041. Higher Surface Energy of Free Nanoparticles. Physical Review Letters, 2003, 91, 106102. 361 Evaporation of Free PbS Nanoparticles: Evidence of the Kelvin Effect. Physical Review Letters, 2002, 89, 190 7.8 105 256103. Liquid-drop model for the size-dependent melting of low-dimensional systems. Physical Review A, 2002, 191 540 One-Dimensional Quantum Confinement in Electrodeposited PbS Nanocrystalline Semiconductors. 192 21.0 79 Advanced Materials, 2001, 13, 280-283. Energy Levels in Embedded Semiconductor Nanoparticles and Nanowires. Nano Letters, 2001, 1, 605-611. 9.1 84 Self-assembled heterojunction between electrodeposited PbS nanoparticles and indium tin oxide 194 3.3 31 substrate. Applied Physics Letters, 2001, 79, 2743-2745. Visible light emission from CdS nanocrystals. Journal Physics D: Applied Physics, 1999, 32, 2306-2310. 2.8 Interface characterization of nanocrystalline CdS/Au junction by current–voltage and 196 2.528 capacitance–voltage studies. Journal of Applied Physics, 1999, 85, 3666-3670. Synthesis Conditions and Superconductivity in 123-Type Superconductors. Journal of 0.5Superconductivity and Novel Magnetism, 1998, 11, 649-652. Size-dependent melting of small particles: a classical approach. European Journal of Physics, 1998, 19, 198 0.6 18 471-472.

#	Article	IF	CITATIONS
199	Electrical properties of 1N4007 silicon diode. Review of Scientific Instruments, 1997, 68, 2904-2908.	1.3	8
200	The temperature dependence of the forward characteristics of 1N4007 silicon diode. Review of Scientific Instruments, 1994, 65, 3289-3290.	1.3	11
201	Group III-Nitrides and Their Hybrid Structures for Next-Generation Photodetectors. , 0, , .		2
202	Pulsed Laser Deposition of Transition Metal Dichalcogenides-Based Heterostructures for Efficient Photodetection. , 0, , .		2
203	Dependence of defect structure on In concentration in InGaN epilayers grown on AlN/Si (111) substrate. Materials Advances, 0, , .	5.4	0